

Technical Note Manual (WEB)

This manual contain an accumulation of knowledge gained by addressing real situations in the field. Many thanks to our customers in the automotive and metal industries for bringing their ideas and concerns to our attention. We are committed to addressing any future concerns as we have done since the incorporation of FMTI Systems Inc., November 13, 1998

Version 3, August 26, 2021

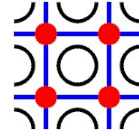
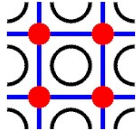
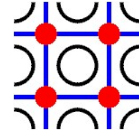
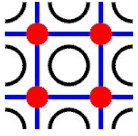


Table of Contents

Table of Contents	2
Measurement Accuracy	3
Exporting Project Data to a Text File	15
Strain Analysis Report Page	18
Fracture Measurements Using Grid Stitching.....	19
Material Thickness (Volume metric Calculation).....	20
Thinning analysis	21
FLC Determined using a Formula Based on Statistical Analysis- Analytical Method –.....	23
Effect of the FMTI Grid Analyzer position on the measurement error	24
<i>Introduction</i>	24
<i>Description of the experiment</i>	24
<i>Conclusions</i>	27
Interpretation of Deformation Measurements for Multiple Operation Processes using TTT or IPD	28
Introduction	28
TTT application.....	30
IPD application.....	34
Model 200 option SGA2x.....	37
Implication Regarding the Usage of a 5mm Circle Grid	39



Measurement Accuracy

The accuracy of the strain measurements can be to +/- 0.5% in the engineering strain measure. However the accuracy depends on the quality of the grid itself. Typically if a roller is used during the electro-etching process with the silk screen, the stencil is stretched in one direction by about 2% which affects the accuracy of the deformation measurements with standard circle (CGA) or square (SGA) grid analysis techniques. Our Tic-Tack-Toe grid analysis option eliminates the initial grid imperfection error and allows the use of a grid scribbled by hand.

Recently one of our customers requested a test of the system accuracy for good quality square grid samples. The following are excerpts from the communication on this subject:

1. Request from the customer

"...I shipped 3 samples to you for analysis as we had discussed. I have marked in red boxes a single area for analysis on each sample. The actual grids to be analyzed contain little pencil dots in them. If the pencil dot interferes with the measurement process please feel free to erase them. If you do this, please find a different way of identifying the grids you measure (i.e. separate map).

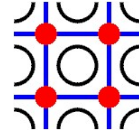
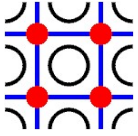
If it isn't too much work, I propose the following (please call me if you disagree). Image all the grids on all the samples once. Base your strain measurements on an initial undeformed grid width of 2.79 mm

Select a single grid on each of the samples (3 grids in total) and measure the single grid 30 times. This should give me a sense of the repeatability of the process...

2. Our reply with the results

"...I have attached six files pertaining to the grid measurement experiment. The files in the pdf format summarize the results graphically. The MS Excel type files contain the strain data in the computer readable digital format. The measurements were completed using ... (both models) ... of the grid analyzer. As the material type, we applied the generic aluminum included with the grid analyzer. On the FLD's generated by the system, the forming severity colour tags (red, yellow and green) are automatically evaluated based on the FLC provided by the generic material. The operator can replace this feature with a manual override, which is more suitable for the FLC generation. However, as the purpose of this experiment was evaluation of the measurement accuracy, we did not change the default settings of the system... "

With the permission of our customer the following pages provide the details of this test for samples 1, 2 - obtained using the camera model 100U and sample 3 - obtained using camera model 100A.



Sample 1

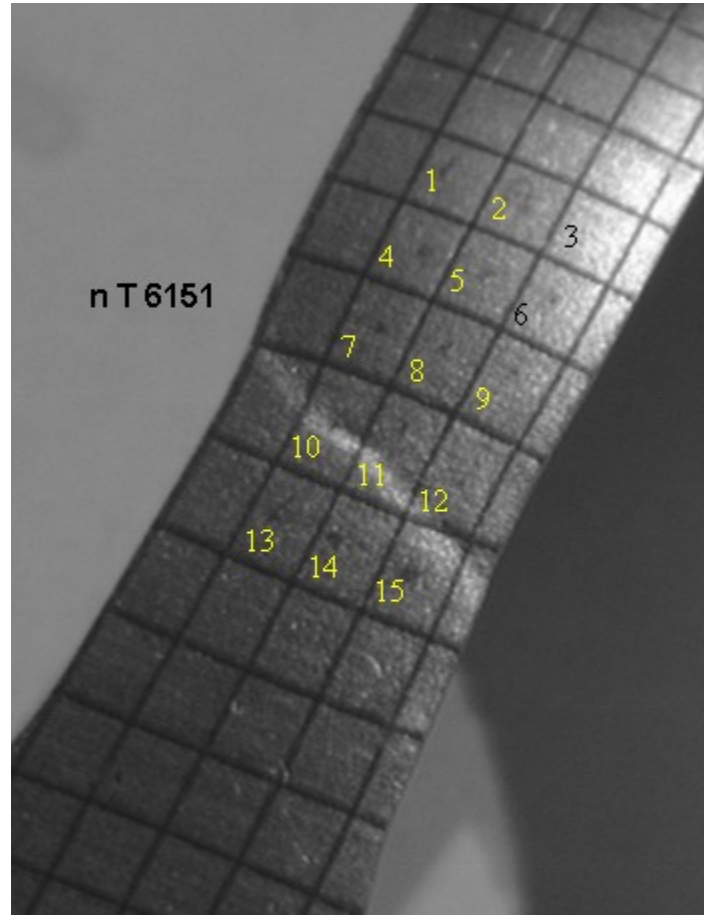
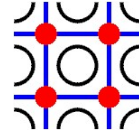
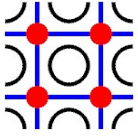


Fig. 1.1u Layout of 15 grid elements

Table 1.1u - strain measurements - one sample per grid only (no averaging)

Grid ID	Major engineering % strain	Minor engineering % strain	Thickness engineering % strain
1	15.5	-3.8	-10.0
2	16.0	-4.9	-9.4
3	16.5	-4.0	-10.5
4	19.7	-5.9	-11.3
5	20.1	-5.9	-11.5
6	20.3	-6.2	-11.4
7	27.1	-9.6	-13.0
8	28.4	-8.8	-14.6
9	28.1	-9.8	-13.4
10	46.6	-14.2	-20.5



11	47.6	-14.1	-21.2
12	40.5	-13.3	-17.9
13	32.8	-11.7	-14.7
14	32.7	-10.9	-15.4
15	34.5	-12.5	-15.1

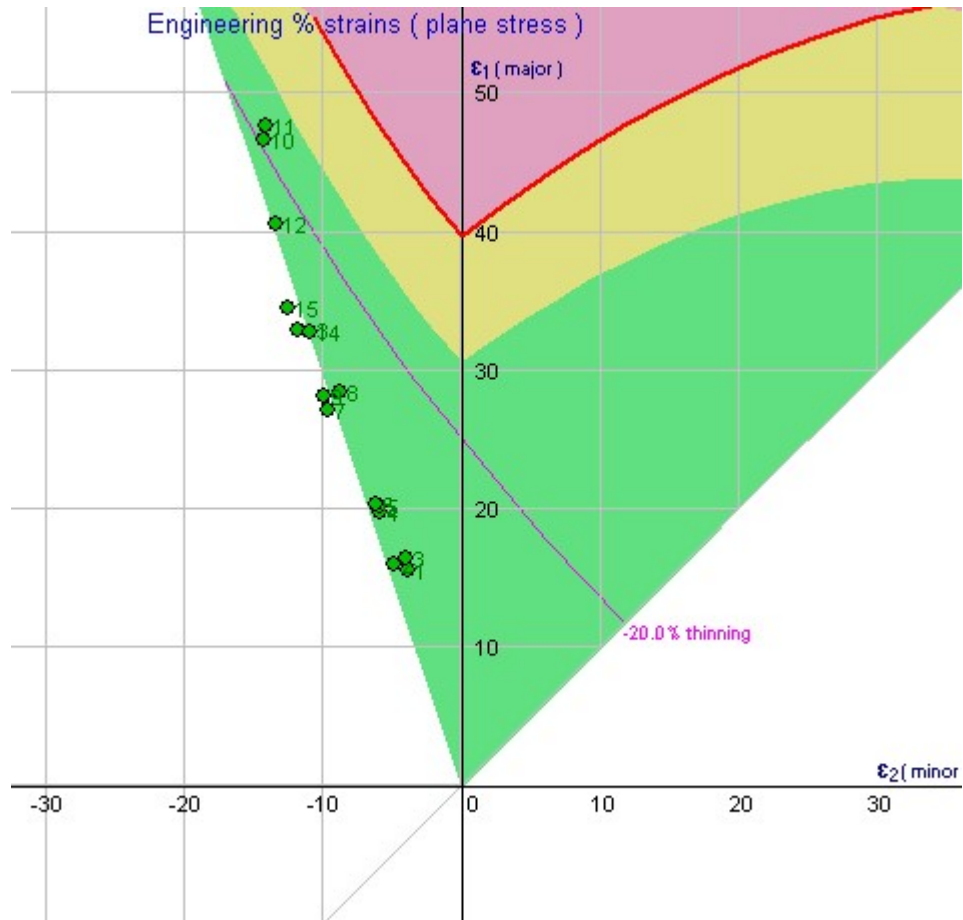
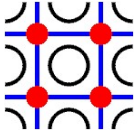


Fig. 1.2u FLD with strain data for sample 1



FMTI Systems Inc.

“Forming Measurement Tools Innovations”

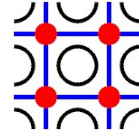
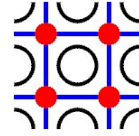
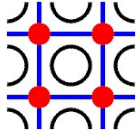


Table 1.2u - strain measurements - sample 1, grid #5 measured thirty times one sample only per entry

Count	Major engineering % strain	Minor engineering % strain	Thickness engineering % strain
1	20.2	-5.6	-11.9
2	19.7	-5.6	-11.5
3	20.0	-5.9	-11.5
4	19.8	-5.8	-11.4
5	19.9	-5.9	-11.3
6	19.6	-5.7	-11.4
7	19.8	-5.7	-11.5
8	19.6	-5.8	-11.3
9	20.0	-5.8	-11.6
10	19.6	-5.8	-11.3
11	19.7	-5.7	-11.4
12	19.7	-5.7	-11.4
13	19.8	-5.8	-11.4
14	19.6	-5.7	-11.3
15	19.6	-5.8	-11.2
16	19.9	-5.9	-11.4
17	20.0	-5.8	-11.6
18	19.8	-5.8	-11.4
19	19.7	-5.7	-11.4
20	19.9	-5.7	-11.6
21	20.2	-5.9	-11.6
22	19.8	-5.7	-11.5
23	19.8	-5.7	-11.5
24	19.7	-5.7	-11.4
25	20.0	-5.9	-11.5
26	19.8	-5.7	-11.5
27	19.6	-5.7	-11.3
28	19.7	-5.5	-11.5
29	19.9	-5.7	-11.5
30	19.9	-5.8	-11.5



Sample 2

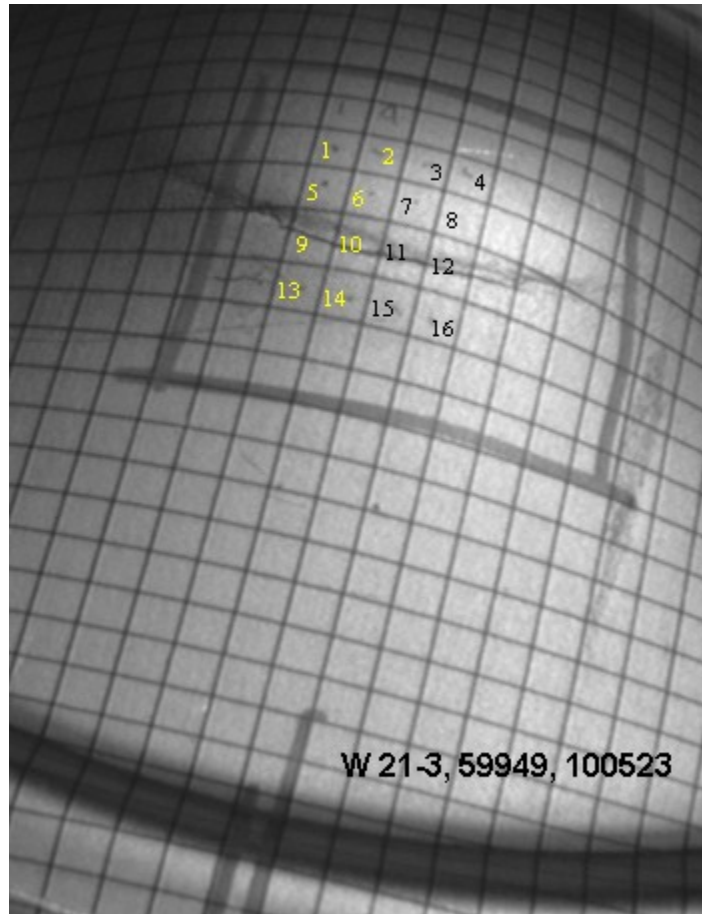
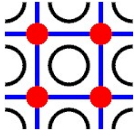


Fig. 2.1u Layout of 16 grid elements



FMTI Systems Inc.

“Forming Measurement Tools Innovations”

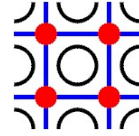


Table 2.1u - strain measurements - one sample per grid only (no averaging)

Grid ID	Major engineering % strain	Minor engineering % strain	Thickness engineering % strain
1	14.9	2.7	-15.2
2	14.4	2.2	-14.5
3	14.1	2.1	-14.1
4	14.4	2.3	-14.5
5	22.2	2.4	-20.1
6	20.3	1.7	-18.2
7	19.7	1.9	-18.0
8	20.5	2.6	-19.1
9	42.6	1.8	-31.1
10	43.3	1.6	-31.3
11	43.8	1.6	-31.6
12	43.1	1.9	-31.4
13	18.3	1.3	-16.6
14	19.9	1.4	-17.8
15	20.5	1.0	-17.8
16	19.7	1.4	-17.7

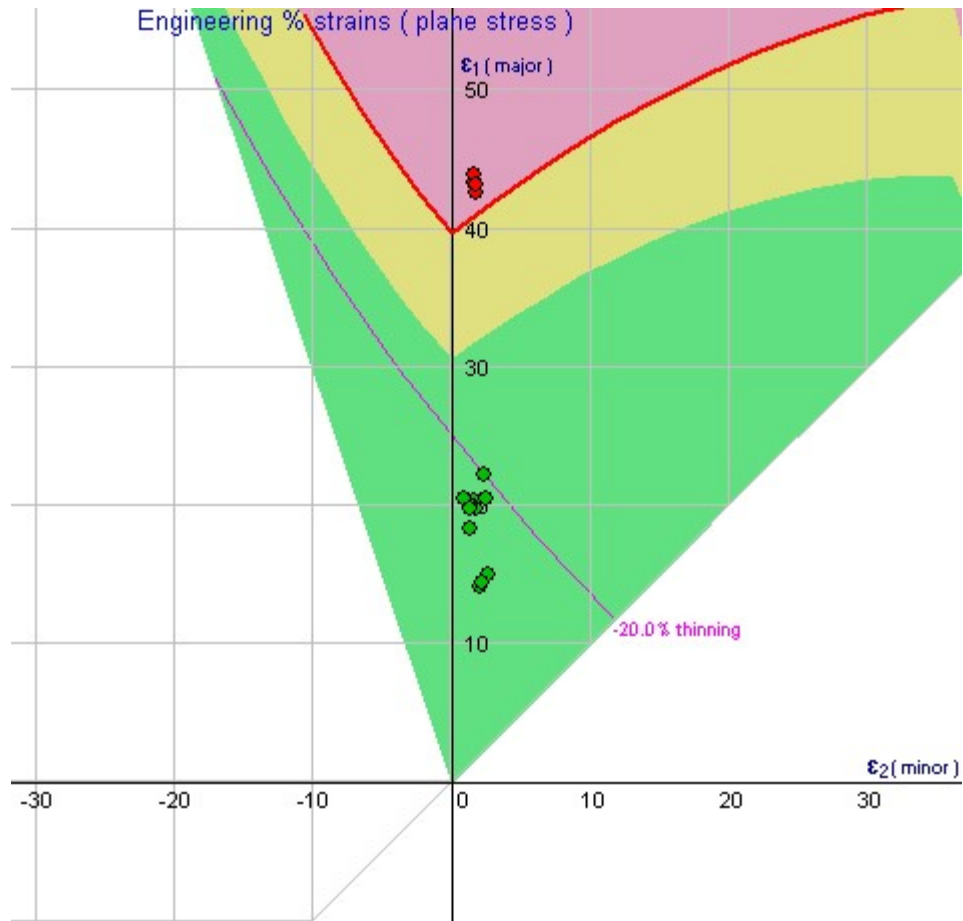
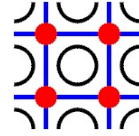
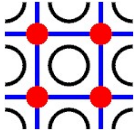
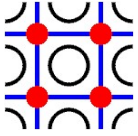


Fig. 2.2u FLD with strain data for sample 2



FMTI Systems Inc.

“Forming Measurement Tools Innovations”

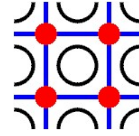
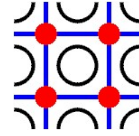
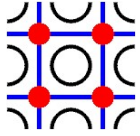


Table 2.2u - strain measurements - sample 2, grid #1 measured thirty times one sample only per entry

Count	Major engineering % strain	Minor engineering % strain	Thickness engineering % strain
1	14.8	2.6	-15.1
2	14.9	2.4	-15.0
3	14.9	2.5	-15.1
4	14.9	2.4	-15.1
5	14.9	2.4	-15.0
6	14.9	2.5	-15.1
7	14.9	2.4	-15.0
8	15.0	2.5	-15.1
9	14.8	2.6	-15.1
10	14.9	2.4	-14.9
11	14.9	2.5	-15.1
12	14.8	2.5	-15.0
13	14.9	2.5	-15.1
14	14.8	2.6	-15.1
15	14.7	2.3	-14.8
16	14.7	2.4	-14.9
17	14.7	2.4	-14.9
18	14.7	2.4	-14.9
19	14.8	2.5	-15.0
20	14.8	2.6	-15.1
21	14.9	2.6	-15.1
22	14.7	2.5	-15.0
23	14.8	2.7	-15.2
24	14.9	2.5	-15.1
25	15.0	2.4	-15.1
26	14.7	2.5	-14.9
27	14.8	2.3	-14.9
28	14.7	2.4	-14.9
29	14.8	2.3	-14.8
30	14.8	2.6	-15.1



Sample 3

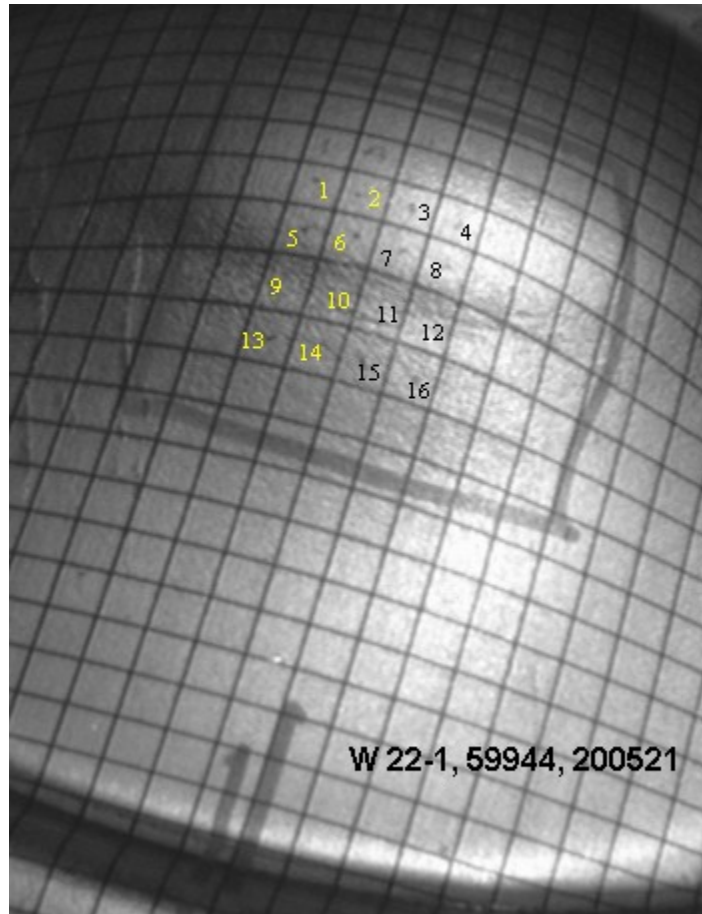
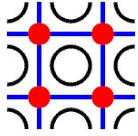


Fig. 3.1 Layout of 16 grid elements



FMTI Systems Inc.

“Forming Measurement Tools Innovations”

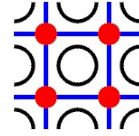


Table 3.1 - strain measurements - one sample per grid only (no averaging)

Grid ID	Major engineering % strain	Minor engineering % strain	Thickness engineering % strain
1	16.2	2.7	-16.2
2	16.1	2.8	-16.2
3	15.6	2.7	-15.8
4	16.4	2.7	-16.4
5	25.0	2.0	-21.6
6	24.1	2.2	-21.1
7	24.2	2.3	-21.3
8	26.3	2.3	-22.6
9	39.1	1.3	-29.0
10	40.1	1.6	-29.8
11	41.6	1.5	-30.4
12	40.5	1.3	-29.8
13	24.8	1.5	-21.0
14	26.1	1.7	-22.0
15	25.0	1.9	-21.5
16	24.9	1.9	-21.4

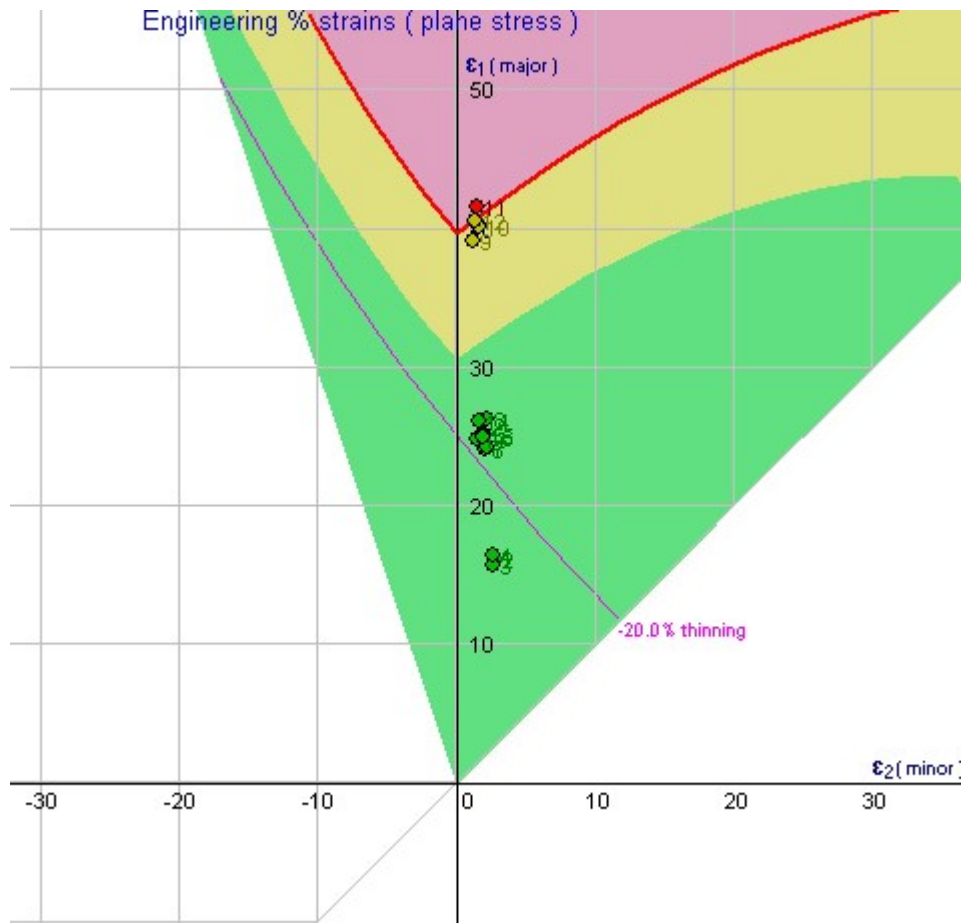
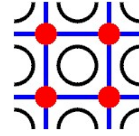
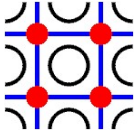
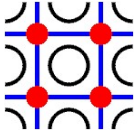


Fig. 3.2 FLD with strain data for sample 3



FMTI Systems Inc.

“Forming Measurement Tools Innovations”

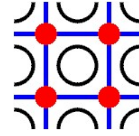
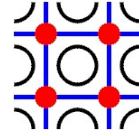
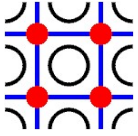


Table 3.2 - strain measurements - sample 3, grid #1 measured thirty times one sample only per entry

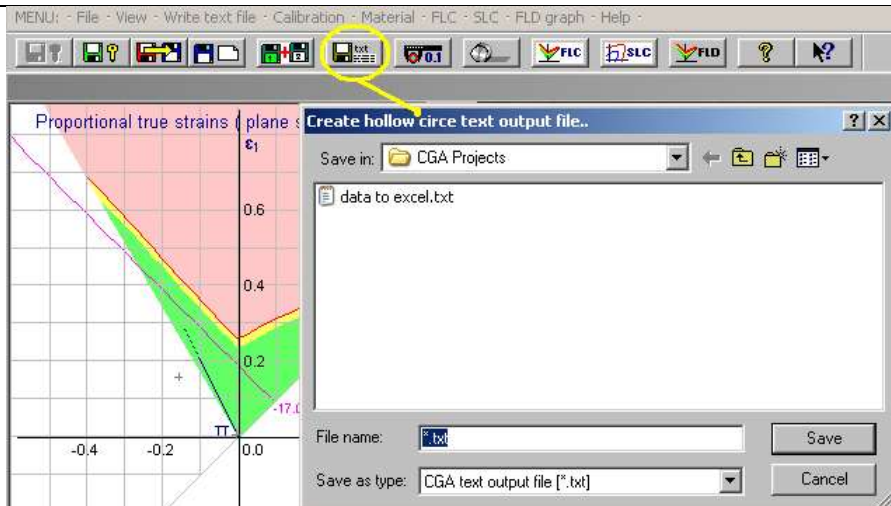
Count	Major engineering % strain	Minor engineering % strain	Thickness engineering % strain
1	16.5	2.7	-16.4
2	16.5	2.7	-16.4
3	16.6	2.7	-16.5
4	16.4	2.8	-16.4
5	16.5	2.7	-16.4
6	16.5	2.7	-16.5
7	16.5	2.7	-16.4
8	16.5	2.8	-16.5
9	16.5	2.8	-16.5
10	16.5	2.7	-16.4
11	16.5	2.7	-16.4
12	16.5	2.7	-16.4
13	16.7	2.7	-16.6
14	16.7	2.7	-16.6
15	16.6	2.8	-16.6
16	16.7	2.7	-16.5
17	16.7	2.7	-16.6
18	16.8	2.7	-16.6
19	16.8	2.6	-16.6
20	16.8	2.7	-16.6
21	16.6	2.7	-16.5
22	16.7	2.8	-16.6
23	16.6	2.7	-16.5
24	16.6	2.7	-16.5
25	16.4	2.8	-16.4
26	16.7	2.7	-16.6
27	16.7	2.8	-16.6
28	16.7	2.7	-16.5
29	16.5	2.7	-16.4
30	16.5	2.7	-16.4



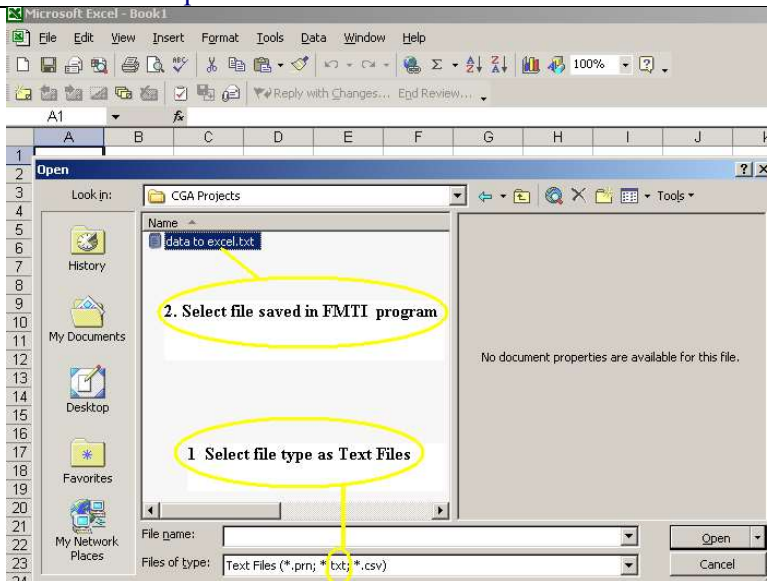
Exporting Project Data to a Text File

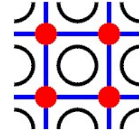
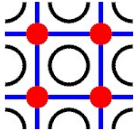
The FMTI Systems grid Analyzer data files may be exported to an ASCII file, which can then be imported by programs such as Microsoft Excel®. This technical note describes the process of exporting the project data from the FMTI CGA and importing the data into Microsoft Excel®.

1.
 - a- Use the txt button in the FMTI Measurement window to create a ASCII text file.
 - b- Select a File name and click on Save.

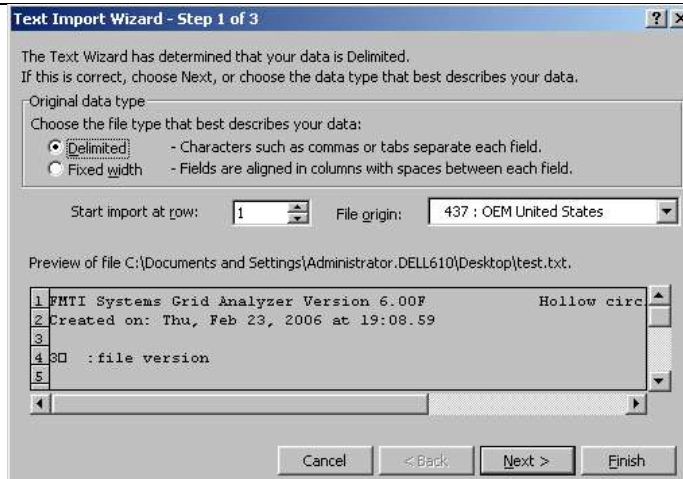


2.
 - a- Open Microsoft Excel® and select File, Open.
 - b- In the Files of Type selection box, select Text Files.
 - c- Select the file saved in step 1.

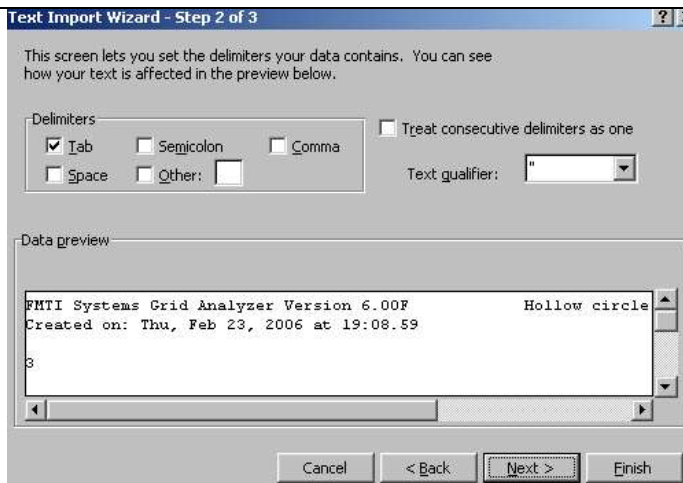


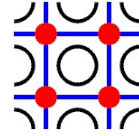
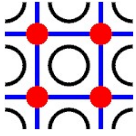


- 3.
- a- The text import wizard will start.
 - b- All the default setting may be used.
 - c- Press Next.

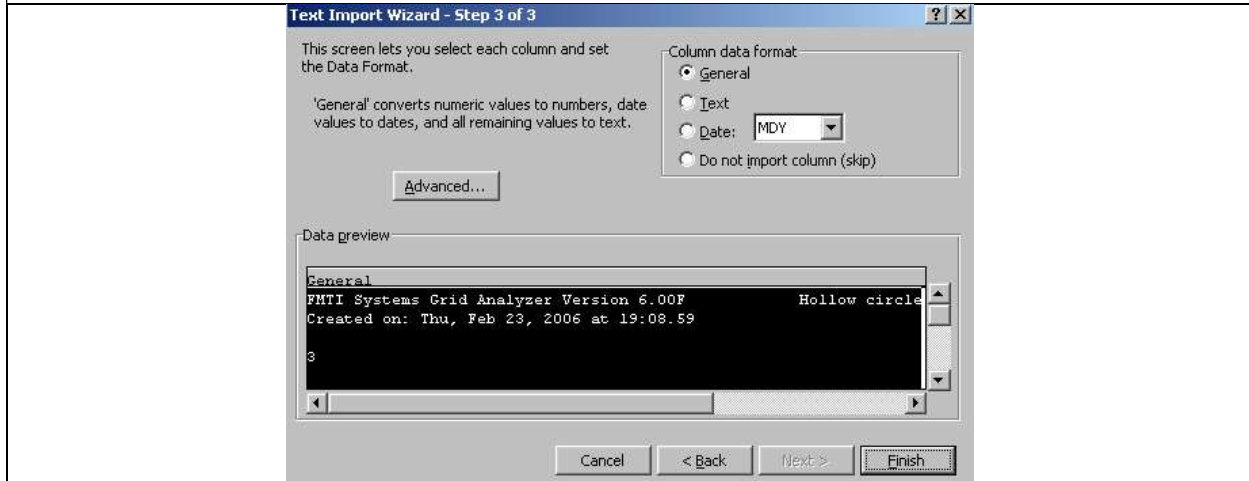


- 4.
- a- Continue with the Text Import Wizard
 - b- Use default settings.
 - c- Press next.

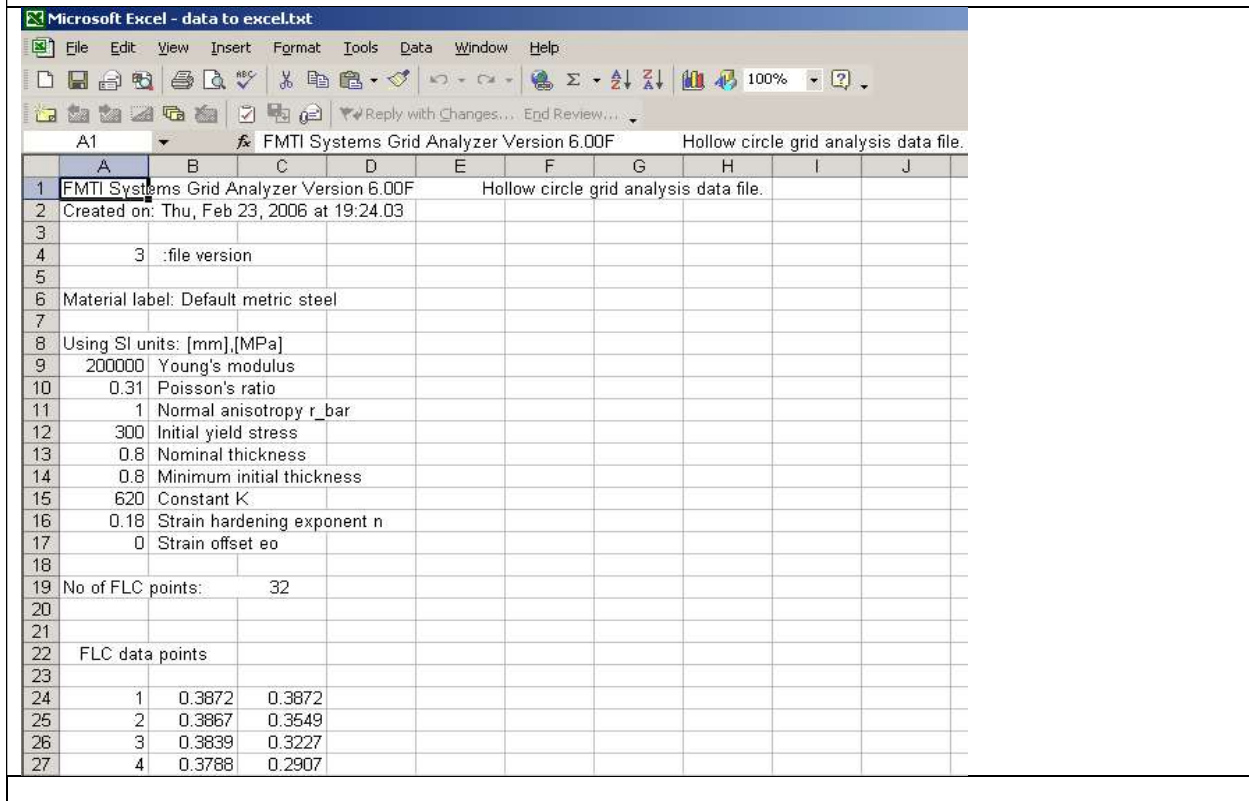


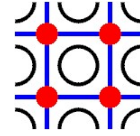
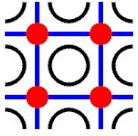


- 5.
- a- Continue with the Text Import Wizard
 - b- Use default settings
 - c- Press finish.



- 6.
- a- All project data is now imported into excel®
 - b- Example below show only a portion of the file. All strain is included in the data file.





Strain Analysis Report Page

The Strain Analysis Report page is provided in either customary or scientific formats. The customary report option generates the strain analysis report page in a format based on the procedures currently used in the automotive and steel industries. The customary forming limit diagram, FLD, provides a plot of the strains with reference to the forming limit curve, FLC. The strains are expressed in the engineering percent strain measure, %e. Simultaneously, the strain data are represented in the form of a table, which includes additional information pertaining to sheet thinning, severity assessment and grid identification. The graph and table displays are synchronized using the left mouse click. The most severely deformed point in the entire data set is automatically selected and highlighted. The assessment of forming severity is based on the current practice, used in production applications, which utilizes the magnitude of the major strain only.

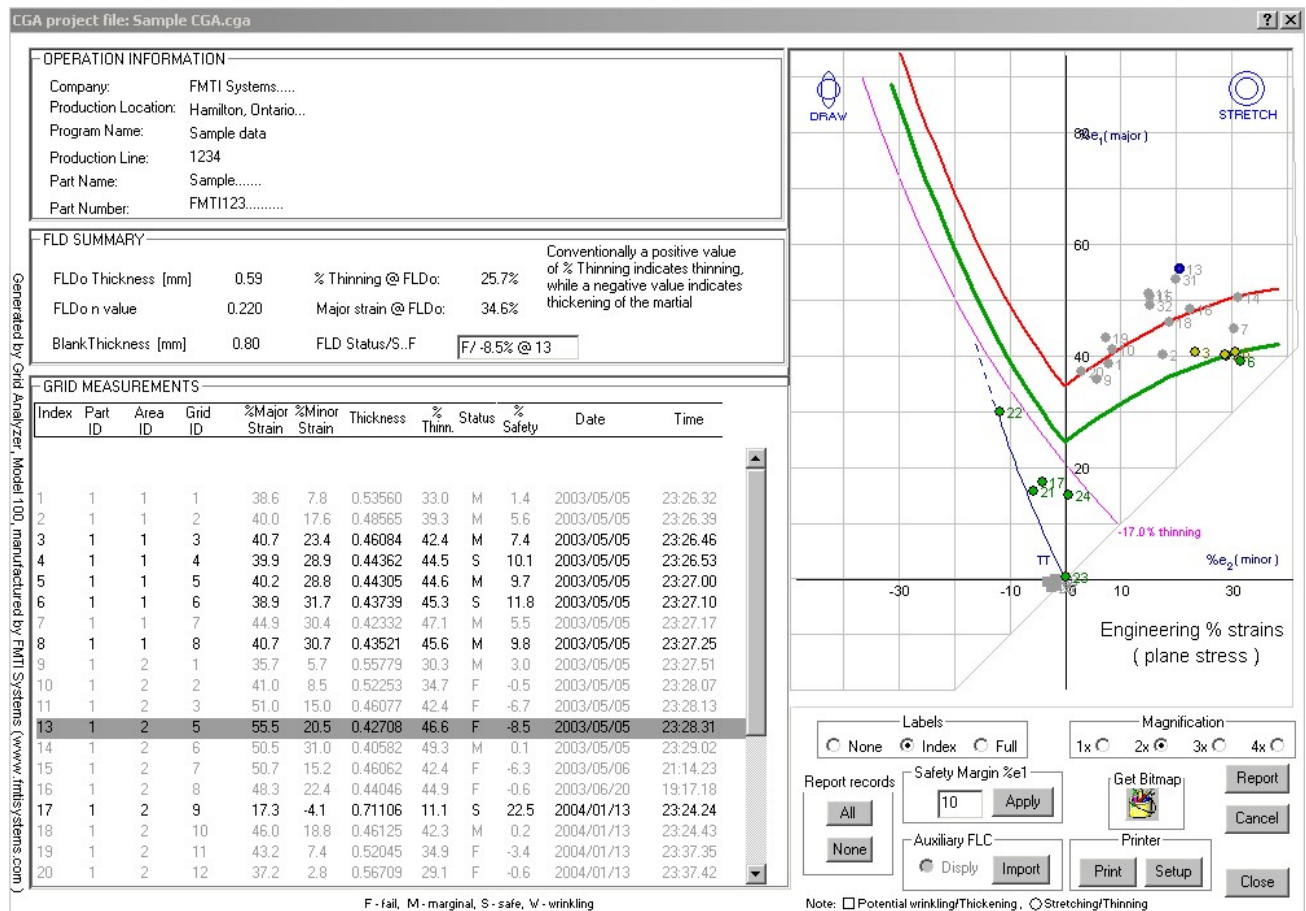
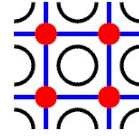
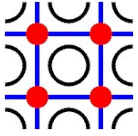


Fig. 1 Example of customary strain analysis report page

The scientific format of the FLD provides similar output to the customary FLD. However, the severity of deformation is calculated based on the proportional deformation, i.e. it utilizes, simultaneously, the magnitudes of both strains, major and minor. This is different than in the case of the customary page, in which the severity is assessed, based on the major strain only. The scientific FLD utilizes either true strains, ϵ , or engineering percent strains, %e.



Fracture Measurements Using Grid Stitching

The grid analyzer provides the grid stitching function, which allows measurement of the fracture strains and tracking the fracture type: necking, normal rupture or shear. The grid stitching function removes the fracture gap running through the grid element before the strain measurements are performed on the digital image of the grid.

The screenshot displays the FMTI software interface with three main components: a camera view on the left, a central data window, and a grid analysis window on the right.

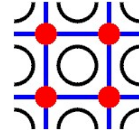
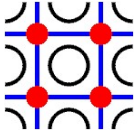
- Step 1:** Shows the initial camera view of a grid pattern on a metal surface.
- Step 2:** Shows the grid stitching process, with red lines indicating the removal of a fracture gap from the grid element.
- Step 3:** Shows the final grid analysis window with a yellow circle highlighting a fracture area labeled "PENDING".

The central data window displays the following information:

- Engineering % strains (plane stress):** A graph showing strain components ϵ_1 , ϵ_2 , and ϵ_3 against shear stress τ . A red circle highlights a point on the graph.
- Plane stress yield locus ($\sigma_y = 300$ MPa):** A graph showing the yield locus with a red circle highlighting a point.
- Fracture data:** A table showing recent strains and fracture data.

Recent strains	ϵ_1	ϵ_2	ϵ_3
Recent	45	48.8%	6.9%
Nominal	0.800	-37.1	

The bottom right corner of the software interface shows a control panel with buttons for "Sample", "REJECT", "Find grid from a first", "Find grid manually", "Process", and "Close".

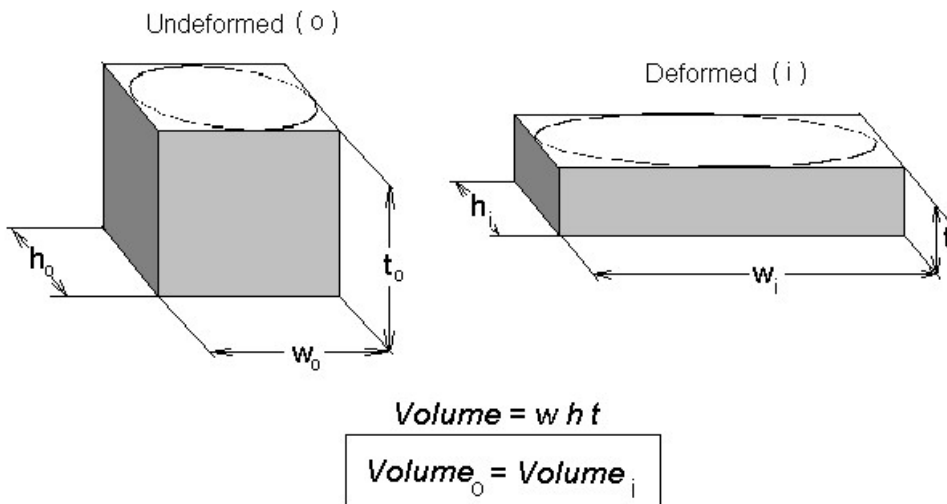


Material Thickness (Volume metric Calculation)

Changes in the material thickness, ε_t , depend on both in plane strains, ε_1 , ε_2 :

$$\varepsilon_t = -\varepsilon_1 - \varepsilon_2.$$

Explanation



Constant volume (incompressibility) of the material implies the following relationship between principal plastic strains:

$$\varepsilon_w + \varepsilon_h + \varepsilon_t = 0,$$

where, $\varepsilon_w, \varepsilon_h, \varepsilon_t$, are true (logarithmic) principal plastic strains calculated as:

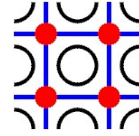
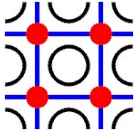
$$\varepsilon_w = \ln\left(\frac{w_i}{w_o}\right), \quad \varepsilon_h = \ln\left(\frac{h_i}{h_o}\right), \quad \varepsilon_t = \ln\left(\frac{t_i}{t_o}\right),$$

and conventionally the major and minor strains used in sheet forming analysis, ε_1 , ε_2 , are defined as:

$$\varepsilon_1 = (\varepsilon_w, \varepsilon_h)_{\max}, \quad \varepsilon_2 = (\varepsilon_w, \varepsilon_h)_{\min}.$$

Proof:

$$\varepsilon_w + \varepsilon_h + \varepsilon_t = \ln\left(\frac{w_i}{w_o}\right) + \ln\left(\frac{h_i}{h_o}\right) + \ln\left(\frac{t_i}{t_o}\right) = \ln\left(\frac{w_i h_i t_i}{w_o h_o t_o}\right) = \ln\left(\frac{Volume_i}{Volume_o}\right) = \ln(1) = 0.$$



Thinning analysis

The ultrasonic gauge measurement of material thinning does not provide a correct assessment of deformation severity. The deformation limit expressed by the conventional forming limit curve, FLC, and the thinning limit of the material can be equated only for the strain states represented by the left side, not the right side, of the forming limit diagram, FLD. This is indicated by the parallel shift between the FLC and the constant thinning lines on the left side of the FLD and diversion of the lines on the right side of the FLD as shown in figure 1. For the strain states represented by the right side of the FLD, the thinning line significantly underestimates the safe deformation limit of the material set by the FLC.

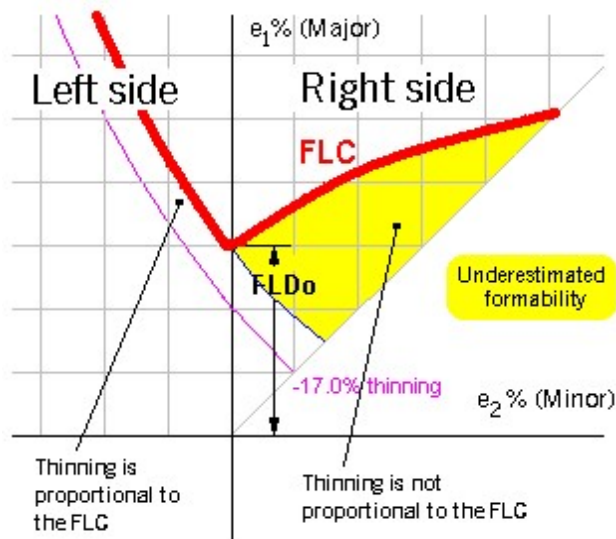


Fig. 1 Forming limit diagram

Furthermore, in order to determine whether or not the thinning of the material represents a valid forming severity measure, i.e. the left side of the FLD, at least one of the surface strains - usually the minor strain - has to be measured to complement the thickness measurement.

An in-plane shear deformation of a sheet has no effect on the sheet's thickness. A sheet material may exhibit fracture failure due to the in-plane shear without any significant changes in thickness. This type of failure is usually observed in high strength materials or in the strain hardened zones of a sheet metal component. Figure 2 illustrates an example of fracture, which occurred in the flat flange and die radius zones of a sheet component, caused by in-plane shear deformation. The fractured area of the sheet component shown in figures 2 exhibits large in-plane shear strains but very small changes in thickness. The presence of an in-plane shear deformation is indicated by surface strains of opposite signs. The surface strains of opposite sign cancel their individual effect on the sheet thickness. This type of critical in-plane shear deformation cannot be detected by the thickness measurements, as the thickness of the material subjected to in-plane shear may remain almost unchanged.

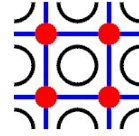
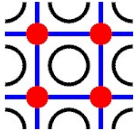
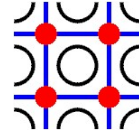
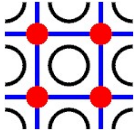


Fig. 2 Shear fracture

In multiple operation processes, such as hydroforming, progressive die or transfer press forming, each operation may produce different surface strains. These different surface strains may or may not change the thickness of the material. This is a similar condition to the case of shear failure as presented in section 2. Essentially, the ductility of the material may be exhausted by applying deformation paths, which do not change the thickness.

Conclusion:

Thinning analysis cannot be used to evaluate forming severity if only one of the three principal strain components, mainly the thickness strain, is being measured. Proper evaluation of forming severity must include all three principal strains.



FLC Determined using a Formula Based on Statistical Analysis- Analytical Method –

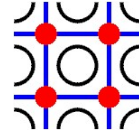
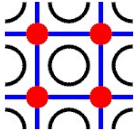
Stuart Keeler and William Brazier¹¹ have developed the following formula for FLC generation based on the statistical data collected for deep drawing quality (DQ) steels:

$$\begin{aligned} & \text{if } (e_2 \geq 0) \{ \\ & \quad e_1 = FLD_0 + e_2 (0.784854 - 0.008565 * e_2) \\ & \quad \text{else} \{ \\ & \quad \quad e_1 = FLD_0 + e_2 (0.027254 * e_2 - 1.1965) \\ & \quad \} \\ & \} \end{aligned} \tag{1}$$

$$FLD_0 = \frac{n}{0.2116} (23.25 + 356.1 * C_1) \tag{2}$$

$$\text{if } (t_0 \leq 0.0118) \{ C_1 = t_0 \} \text{ else } \{ C_1 = 0.0118 \} \tag{3}$$

where, t_0 , is the thickness of the undeformed sheet in inches, n is the strain hardening exponent and e_1 and e_2 are points on the FLC expressed as percent engineering strains.



Effect of the FMTI Grid Analyzer position on the measurement error

Introduction

The FMTI grid analysis system performs strain measurement based on the digitization of the grid image projected onto the flat surface of the CCD sensor of a digital camera. Position of the camera, distance of the lens to the grided surface and the curvature of the grided surface affect the shape and magnification of the image.

This document provides the results of an experimental evaluation of the effect of the Grid Analyzer position on the strain measurement error.

Description of the experiment

The experiment was conducted on a 0.1-inch reference square grid using the FMTI Grid Analyzer basic model 100U equipped with the 25 mm lens. The reference grid samples were printed on a white paper using a laser printer. Using a laser-printed grid on paper practically eliminated any initial grid shape imperfections, which are typical for grids produced by the process of electro-etching of sheet metal. The samples of the grid on paper are shown in figure 1 along with the set of metal washers used as spacers in the experiments.

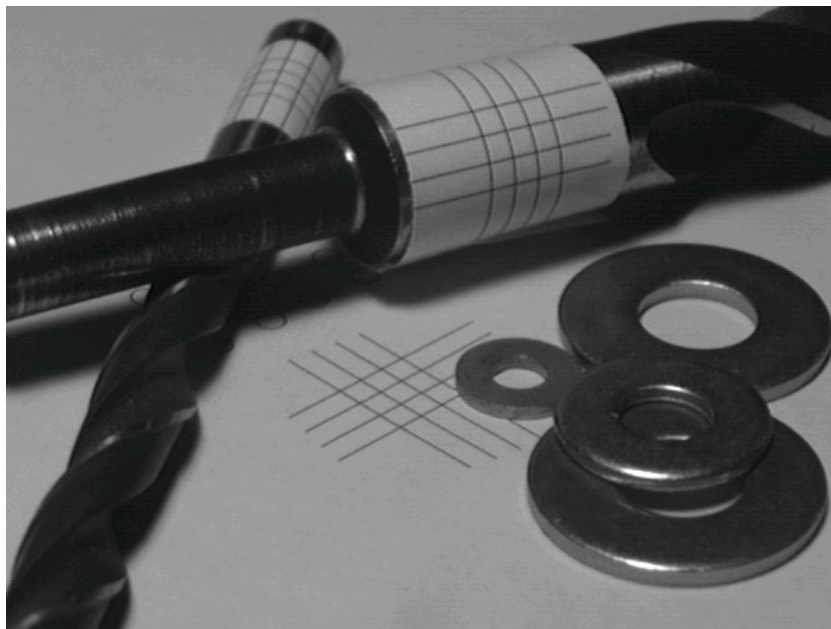
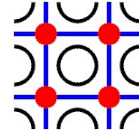
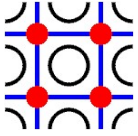


Fig. 1 – paper with 0.1 inch square grid, cylindrical samples and spaces

The grid on the flat paper was used to calibrate the undeformed grid size reference. During the calibration the grid image was positioned in the center of the camera view frame. After the calibration the same undeformed grid was used to measure strains under different conditions. Each measurement was taken



only once. As the grid was not deformed, the measured strains represent the measurement errors introduced by the specific conditions of the test. The following four conditions of the of the measurements were examined:

- 1) off-center position of the grid in the camera view,
 - 2) gap between the camera and the gridded surface,
 - 3) tilt of the camera,
 - 4) curvature of the gridded surface,
- which are discussed below in greater detail.

Effect of the “off-center” position of the grid in the camera view frame

In this experiment the camera’s nose was placed flat on the paper with the grid and three measurements of the grid were taken for the following positions of the grid in relation to the center of the camera’s view frame: a) central position, b) grid shifted South-East and c) grid shifted North-West. Figure 2 illustrates three positions of the flat grid and the recorded values of major and minor engineering percentage strains.

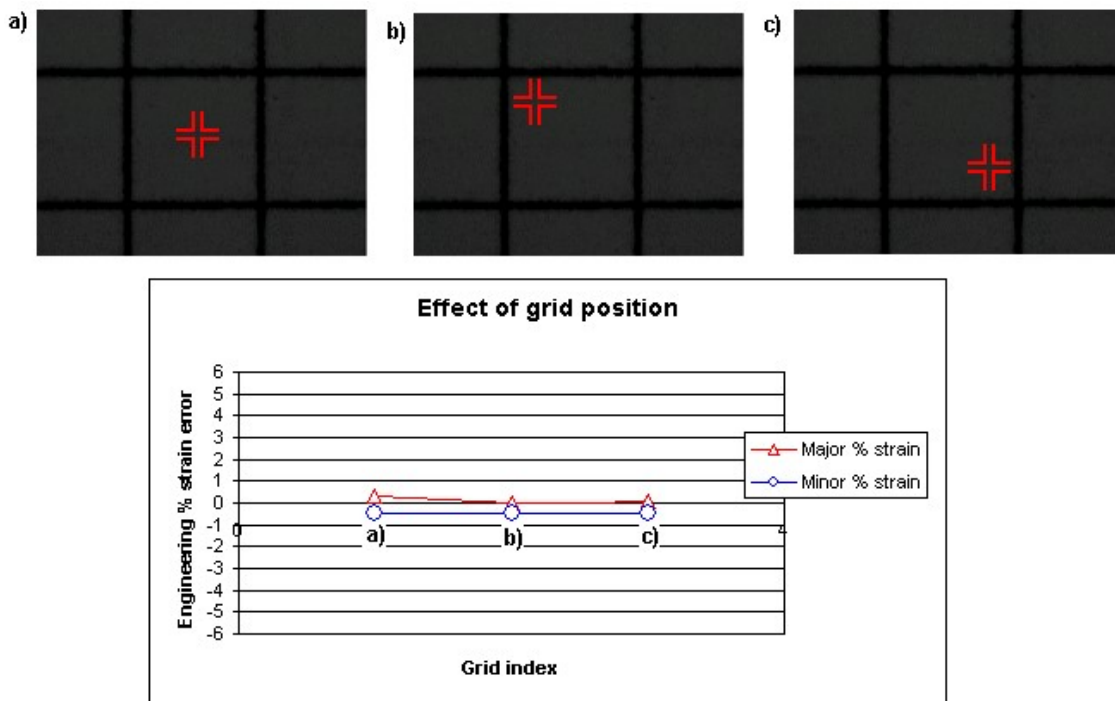
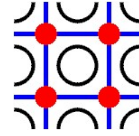
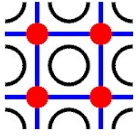


Fig. 2 Effect of the grid position in camera view frame

The range of strains from -0.5% to $+0.3\%$ is the same as the scatter of the initial grid calibration. This indicates that in the case of a flat grid the off center position of the grid has no effect on the measurement error.

- 2) Effect of a gap between the camera and the gridded surface



In this experiment the camera was raised vertically above the grid, by means of spacers placed between the paper with the grid and the nose of the Grid Analyzer. Three different elevations of the camera were applied: 0.035, 0.068, and 0.122 in. The results of this test are shown in figure 3.

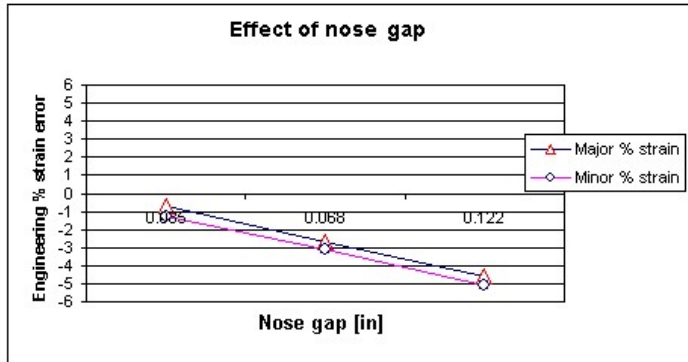


Fig. 3 Effect of a gap between the camera and the gridded surface

This experiment indicates that for a small gap of 0.035 in (~1.0 mm) the gap effect is negligible. However, as the gap (distance of the CCD camera element from the grid plane) increases, the image in the camera view becomes smaller, and the measurement error is revealed as the negative strains. The magnitude of the error approaches the negative value -5% at the distance of 0.122 in, (3.0 mm).

3) Effect of the camera tilt

It is possible that while taking the strain measurements the operator unknowingly tilts the camera from the ideal position perpendicular to the sheet. The effect of the tilt on the measurement error was the subject of this experiment. The grid measurements were performed with one side of the camera nose resting on the flat sheet with the grid while a spacer lifted the opposite side of the nose up. Three different magnitude of the tilt were applied: 0.035, 0.068, and 0.122 in. The results of this test are shown in figure 4.

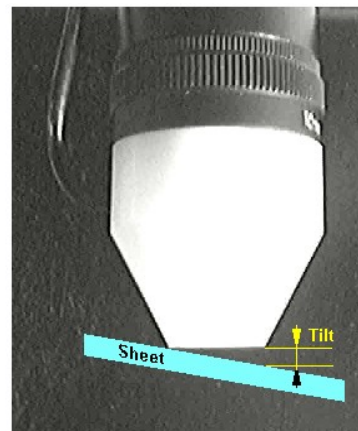
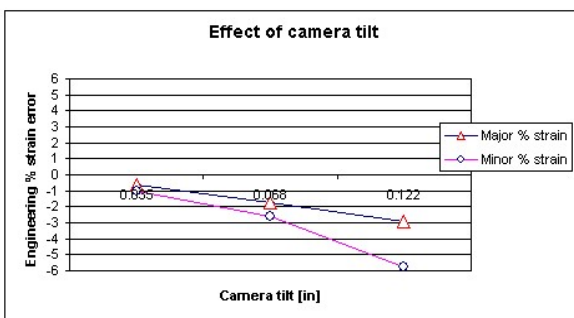
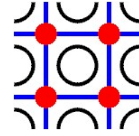
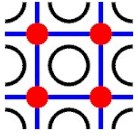


Fig. 4 Effect of the camera tilt



This experiment indicates that for a small tilt of 0.035 in (~1.0 mm) the tilt effect is negligible. However, as the tilt increases, the image in the camera view becomes non-uniformly smaller. The grid distortion increases along the tilted axis direction. As the result of this directional distortion the error represented by the minor strain is more noteworthy as compared with the error represented by the major strain. The magnitude of the minor strain error approaches the value of -6% for a tilt of 0.122 in, (3 mm), while the major strain error is only -3%.

4) Effect of the surface curvature

The effect of the surface curvature was examined using samples of the grid wrapped on cylindrical objects of defined diameter as shown in fig. 1. Three different surface radii were applied: 0.365, 0.185 and 0.125 in. The results of this test are shown in figure 5.

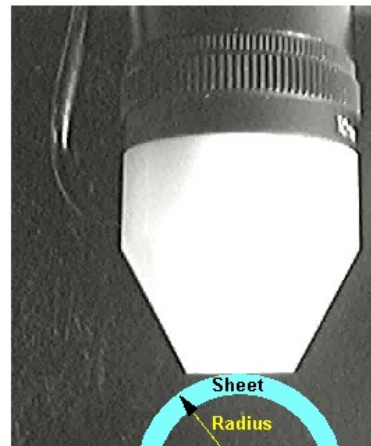
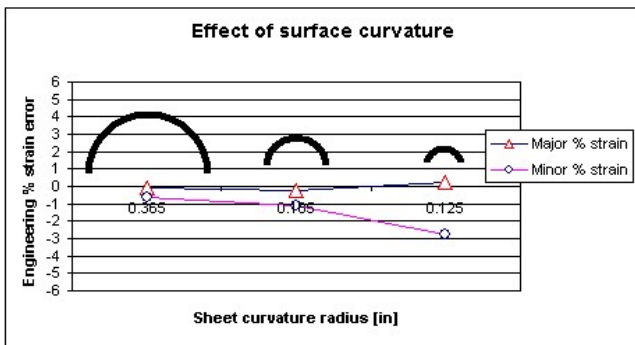


Fig. 5 Effect of surface curvature

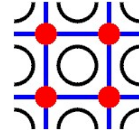
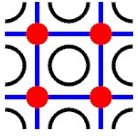
This experiment indicates that the surface curvature introduces only a moderate error of -3% for a relatively sharp radius of 0.125 in. For larger radii the curvature effect is negligible.

Conclusions

As long as the systems operator gives some reasonable attention to the Grid Analyzer perpendicular position to the gridded surface the measurement errors caused by the camera position are relatively small, less than -2% in the engineering percentage strain measure.

The errors due to the Grid Analyzer position reduce the actual magnitude of both principal strains, which results in an underestimation of the tearing failure condition and overestimation of the buckling failure condition.

The results presented in this report refer only to a specific lens and grid size, which are 25mm lens and 0.1 inch grid size.



Interpretation of Deformation Measurements for Multiple Operation Processes using TTT or IPD

Introduction

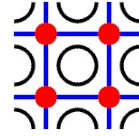
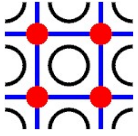
FMTI Systems pioneered the development of the grid analysis technique for multiple operation processes, such as progressive die forming, transfer press forming, and tube hydroforming with pre-form. The main difficulty in the analysis of multiple operation processes is that the conventional concepts of major-minor strains, $\varepsilon_1 - \varepsilon_2$, and the forming limit diagram, FLD produce ambiguous results. For example, during a hydroforming process of shaping a tubular member, with the tube being pre-formed by bending, the grid elements located at the inner surface of the bend are initially compressed and shortened. During subsequent expansion of the tube by pressurized liquid or gas these elements may return to their initial shape and reach the fracture limit of the material with the apparent strains at a level below the forming limit curve, or even approaching zero magnitude. Similarly, a sheet material stretched in one operation and subjected to compression in the next operation, may exhibit wrinkling contradicting the apparent stretching strain state indicated by a point on the FLD.

Concepts employed in the grid analysis of multiple operation processes

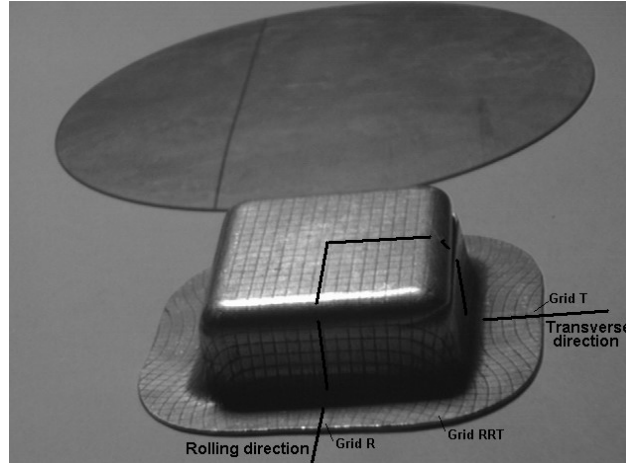
The analysis of multiple operation processes developed by FMTI Systems is based on two fundamental concepts. The first concept is the utilization of directionality of deformation in material space. The material space is referred to by the rolling direction of a sheet or the axial direction of a tube. This concept allows for differentiating between operations, in which the same amount of strain increments when applied in different directions leads to a completely different final shape of the workpiece, for example the plane strain axial elongation of a tube (constant diameter) versus the plane strain expansion of the tube's diameter (constant length). The second concept is the utilization of the stress state for the interpretation of deformation evolution and the assessment of forming severity. The stress state based failure criterion eliminates the ambiguous phenomenon of fracture failure at a near zero strains of an otherwise well deformable material.

Examples of grid analysis for multiple operation processes

The following examples illustrate the interpretation of grid analysis results for multiple operation processes. In order to simplify the subject, instead of using an actual multiple operation process, the examples utilize simple sequences of grid shape changes, taken from different areas of the same part. The sequence of grid images was chosen intentionally to provide data, for which the staged deformation evolution can easily be intuitively interpreted. All examples consist of three simulated operations. The 1st operation changes the initial shape of the undeformed grid. The results pertaining to the 1st operation are equivalent to the results produced by the traditional circle grid analysis, CGA. The 2nd operation simulates a deformation-causing near return of the grid to its initial shape. In this case an image of an undeformed grid was used. Intuitively, the principal directions of deformation should be preserved, but the strains and stresses in the 2nd operation should be opposite to the strains and stresses determined for the 1st operation. Additionally, the overall level of stresses should increase due to the strain hardening of the material. The 3rd operation repeats the deformation induced in the 1st operation. The principal strains and directions

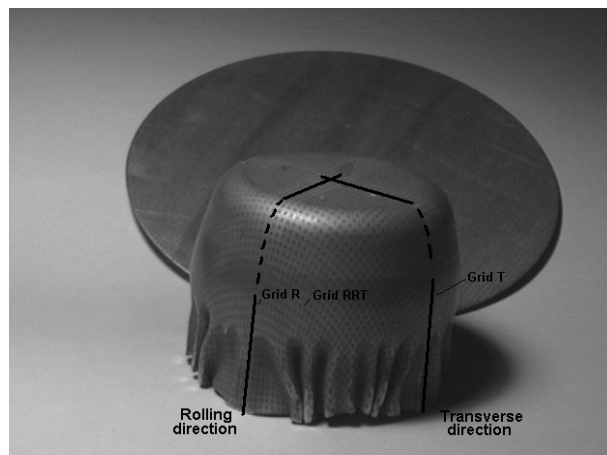


should be similar to those determined for the 1st operation, but the overall level of stresses should exhibit a further increase.



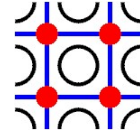
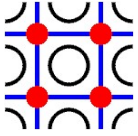
Sample used to generate data for the TTT program.

The data used with the TTT program were produced using a square cup marked with a square grid. Three grid elements located near the edge of the flange were measured to simulate the 1st and the 3rd operation. Nearly undeformed grid elements at the bottom were used to simulate the 2nd operation. The edge of the flange is subjected to uniaxial compression. (negative hoop stress, zero radial stress). Points away from the edge exhibit a gradual increase of radial tension and diminishing of the negative hoop stress.



Sample used to generate data for the IPD program.

The data used with the IPD program were produced using a cylindrical cup marked with the polka dot grid pattern. Three grid elements located in the middle of cup wall were measured to simulate the 1st and the 3rd operation. Nearly undeformed grid elements at the bottom were used to simulate the 2nd operation. The center of the wall is subjected to a combination of axial tension and radial compression (draw deformation). Material points away from the wall center towards the bottom of the cup exhibit a gradual diminishing of the negative hoop stress, while the magnitude of the hoop stress increases toward the



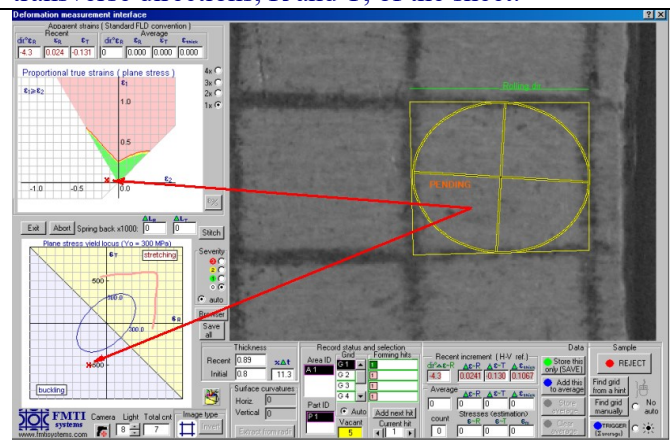
flange. In both examples the 1st operation used a grid, R, along the rolling direction, a grid, T, along the transverse direction and a grid RRT located away from but in proximity to the rolling direction. The 2nd operation is simulated by a nearly undeformed grid located at the bottom of the cup. The 3rd operation used again the grids located in areas R, T, and RRT.

TTT application

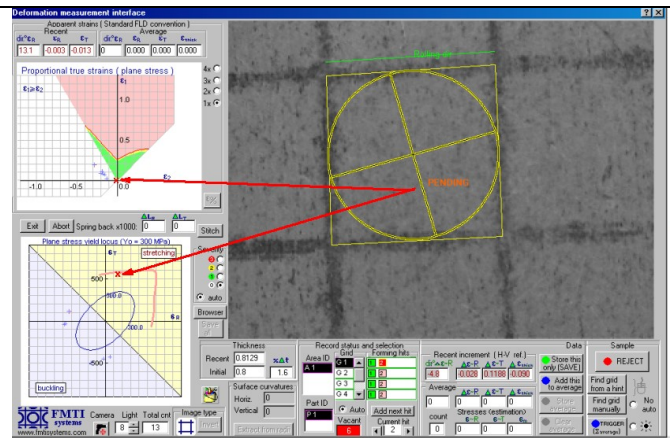
Description of the deformation evolution in three operations for the square grid element, R, located along the rolling direction of the sheet.

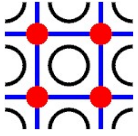
Grid analyzer measurements window with the grid image, the FLD displaying apparent major-minor strains, and the principal stress diagram, $\sigma_R - \sigma_T$, which associates the principal stresses with the proximity of their directions to the rolling and transverse directions, R and T, of the sheet.

1st operation. The grid element is shortened along the transverse direction and slightly elongated along the rolling direction. The strain state consists of both; small positive major strain and negative minor strain. On the FLD the strain state point is located in the wrinkling zone away from the fracture limits set by the forming limit curve, FLC. The stress state consists of a small compressive stress, $\sigma_R \approx 0$, (measurements error) in the rolling direction, and a large compressive stress, $\sigma_T < 0$, acting in the transverse direction.



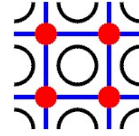
2nd operation. The grid element is nearly deformed back to its original “undeformed” shape. On the FLD the apparent strain state point is: $\epsilon_1 \approx \epsilon_2 \approx 0$. However, the stress state reveals that in order to arrive at this shape of the element from the shape recorded after the 1st operation, the stresses in the 2nd operation are reversed. The stress in the rolling direction remains small, $\sigma_R \approx 0$. However, the grid element is elongated in the transverse direction by a large positive stress, $\sigma_T > 0$, which approaches the fracture stress limit of the material. The overall level of stresses is higher due to the strain hardening of the material.



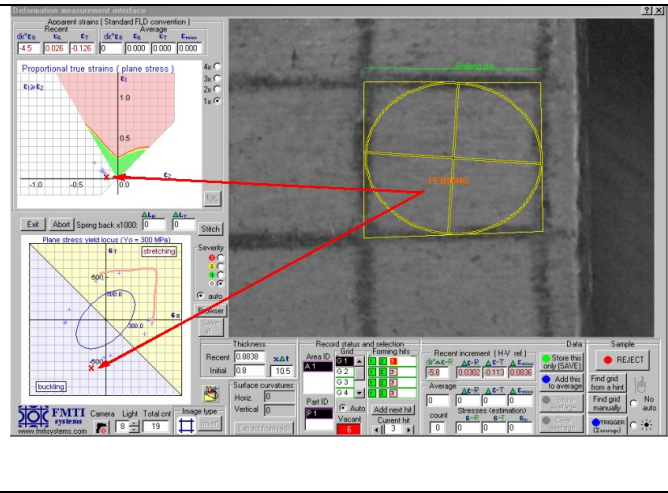


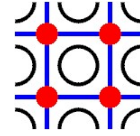
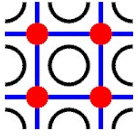
FMTI Systems Inc.

“Forming Measurement Tools Innovations”



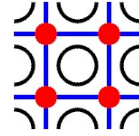
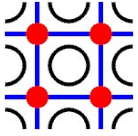
3rd operation. The grid element is again shortened along the transverse direction and slightly elongated along the rolling direction. The strain state consists of a small positive major strain and a negative minor strain. The apparent strain state consists of a small positive major strain and a large negative minor strain, as in the first operation. The stress state shows the same similarity. However, the overall level of stresses is again higher as it reflects the strain hardening effect induced by all three operations.

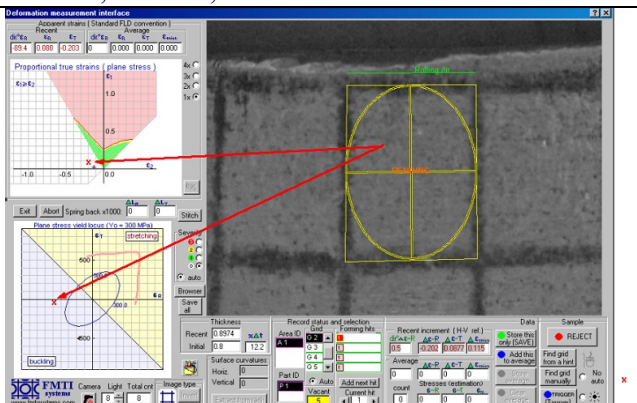
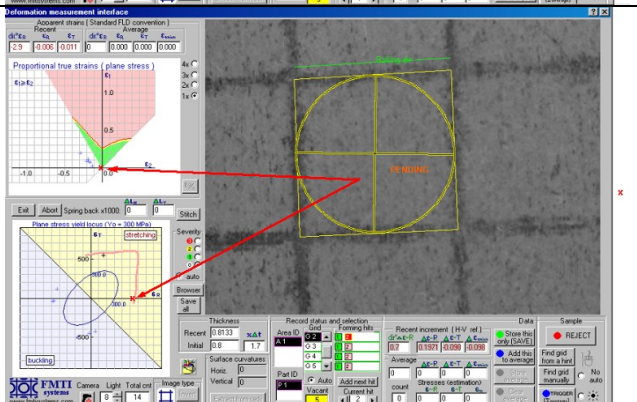
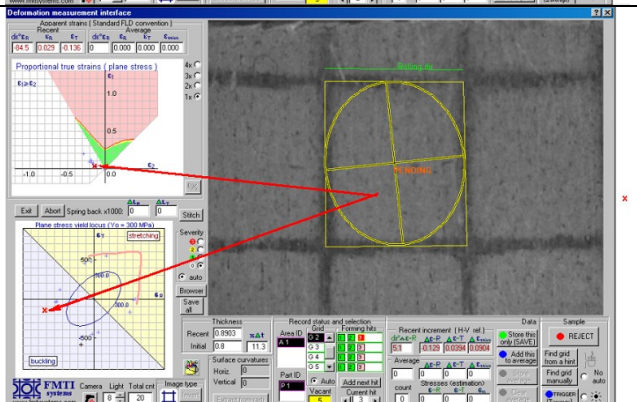


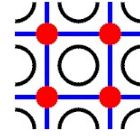
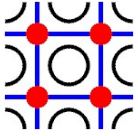


TTT application contd.

<p>Description of the deformation evolution in three operations for the square grid element, RRT, located in proximity to the rolling direction of the sheet.</p>	<p>Grid analyzer measurements window with the grid image, the FLD displaying apparent major-minor strains, and the principal stress diagram, $\sigma_R - \sigma_T$, which associates the principal stresses with the proximity of their directions to the rolling and transverse directions, R and T, of the sheet.</p>
<p>1st operation.</p> <p>The strain and stress state for grid RRT is similar to the one recorded for grid R. The only noticeable difference is that the orientation of principal strains and stresses in material space, is about -30° away from the rolling direction of the sheet.</p>	
<p>2nd operation</p> <p>The strain and stress state for grid RRT is similar to the one recorded for grid R. The only noticeable difference is that the orientation of principal strains and stresses in material space, is about -30° away from the rolling direction of the sheet.</p>	
<p>3rd operation.</p> <p>The strain and stress state for grid RRT is similar to the one recorded for grid R. The only noticeable difference is that the orientation of principal strains and stresses in material space, is about -19° away from the rolling direction of the sheet.</p>	



<p>Description of the deformation evolution in three operations for the square grid element, T, located along the transverse direction of the sheet.</p>	<p>Grid analyzer measurements window with the grid image, the FLD displaying apparent major-minor strains, and the principal stress diagram, $\sigma_R - \sigma_T$, which associates the principal stresses with the proximity of their directions to the rolling and transverse directions, R and T, of the sheet.</p>
<p>1st operation.</p> <p>The strain and stress state for grid T is similar to the one recorded for grid R. The only noticeable difference is that the principal strains and stresses associated with directions, R and T, are exchanged.</p>	
<p>2nd operation</p> <p>The strain and stress state for grid T is similar to the one recorded for grid R. The only noticeable difference is that the principal strains and stresses associated with directions, R and T, are exchanged.</p>	
<p>3rd operation.</p> <p>The strain and stress state for grid T is similar to the one recorded for grid R. The only noticeable difference is that the principal strains and stresses associated with directions, R and T, are exchanged.</p>	



IPD application

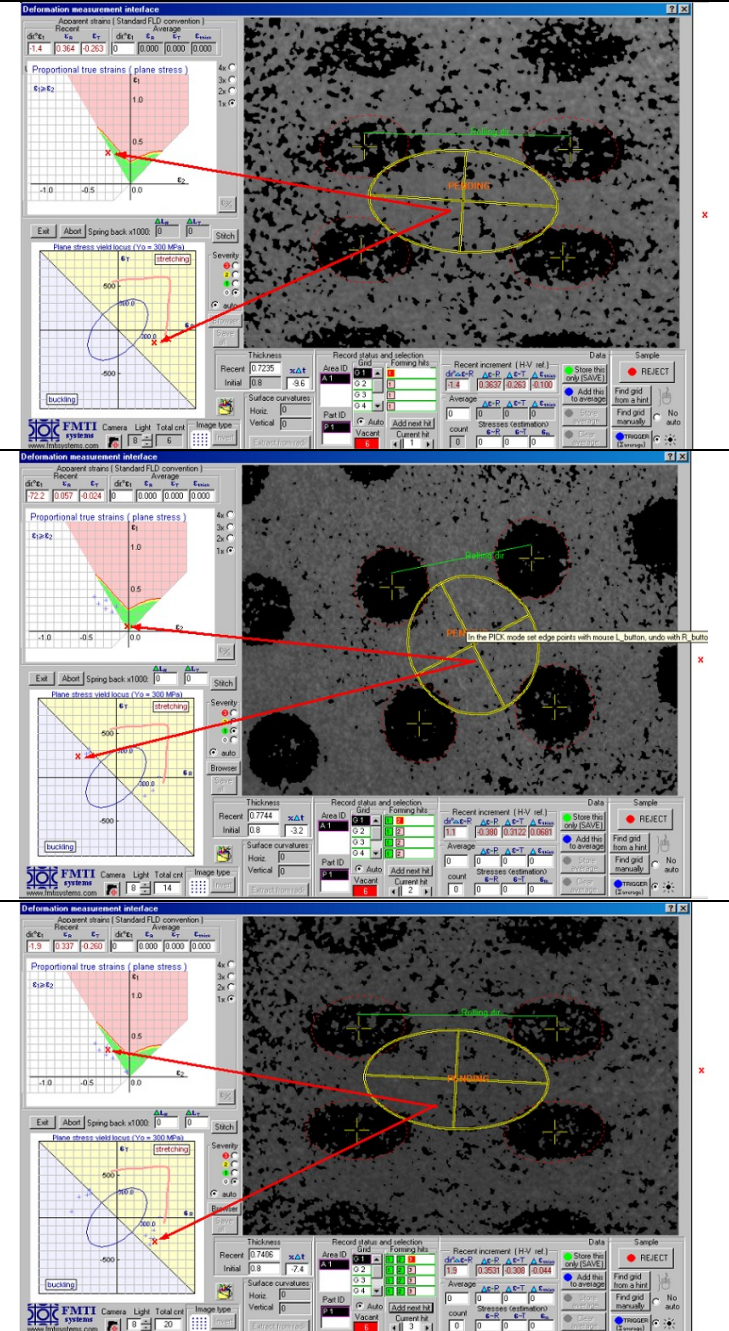
Description of the deformation evolution in three operations for the Polka Dot grid element, R, located along the rolling direction of the sheet.

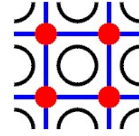
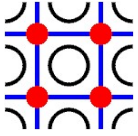
1st operation. The grid element is elongated along the rolling direction and shortened in the transverse direction. The strain state consists of both; positive major strain and negative minor strain. On the FLD the strain state point is located between the paths, $\epsilon_1 = -2\epsilon_2$, representing uniaxial tension and, $\epsilon_1 = -\epsilon_2$, representing the in-plane shear. The stress state consists of tension in the rolling direction, $\sigma_R > 0$, and a small compressive stress, $\sigma_T < 0$, acting in the transverse direction.

2nd operation. The grid element is nearly deformed back to its original “undeformed” shape. On the FLD the apparent strain state point is: $\epsilon_1 \approx \epsilon_2 \approx 0$. However, the stress state reveals that in order to arrive at this shape of the element from the shape recorded after the 1st operation, the stresses in the 2nd operation are reversed. The grid element is now shortened in the rolling direction by a compressive stress, $\sigma_R < 0$, and elongated in the transverse direction by a positive stress, $\sigma_T > 0$. The overall level of stresses is higher due to the strain hardening of the material.

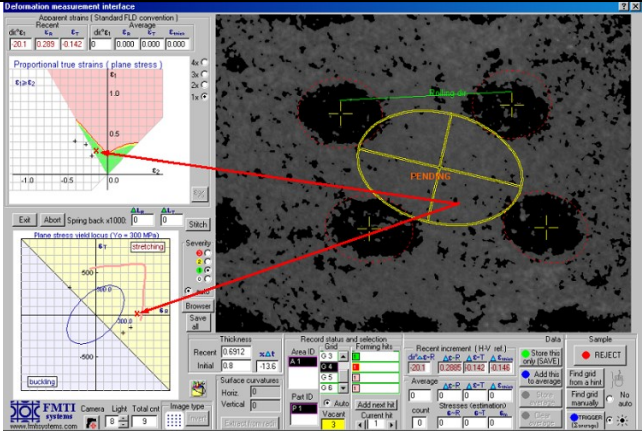
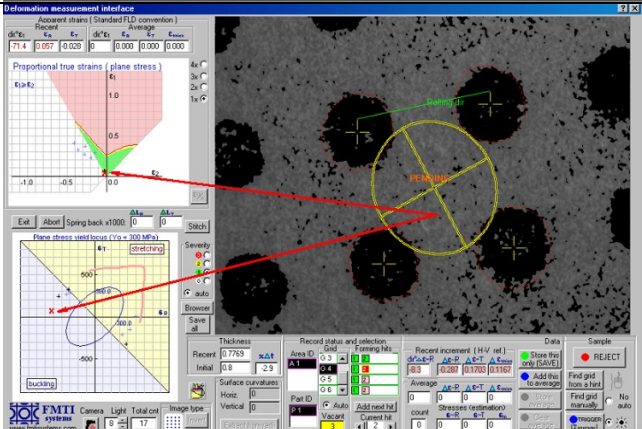
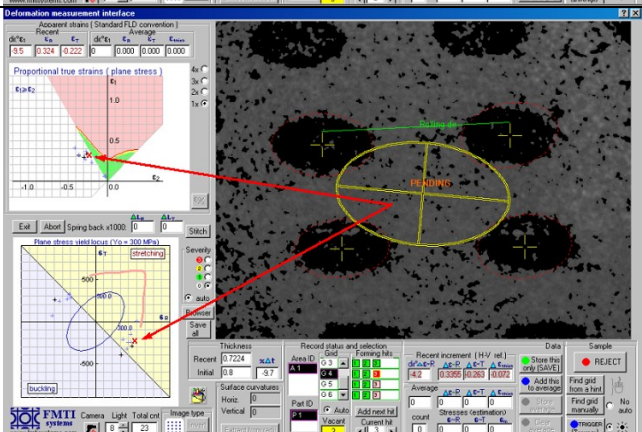
3rd operation. The grid element is again elongated along the rolling direction and shortened in the transverse direction. The apparent strain state consists of a positive major strain and a negative minor strain, as in the first operation. The stress state shows the same similarity. However, the overall level of stresses is again higher as it reflects the strain hardening effect induced by all three operations.

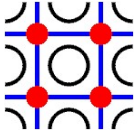
Grid analyzer measurements window with the grid image, the FLD displaying apparent major-minor strains, and the principal stress diagram, $\sigma_R - \sigma_T$, which associates the principal stresses with the proximity of their directions to the rolling and transverse directions, R and T, of the sheet.





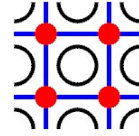
IPD application contd.

<p>Description of the deformation evolution in three operations for the Polka Dot grid element, RRT, located in proximity to the rolling direction of the sheet..</p>	<p>Grid analyzer measurements window with the grid image, the FLD displaying apparent major-minor strains, and the principal stress diagram, $\sigma_R - \sigma_T$, which associates the principal stresses with the proximity of their directions to the rolling and transverse directions, R and T, of the sheet.</p>
<p>1st operation.</p> <p>The strain and stress state for grid RRT is similar to the one recorded for grid R. The only noticeable difference is that the orientation of principal strains and stresses in material space, is about -20° away from the rolling direction of the sheet.</p>	
<p>2nd operation</p> <p>The strain and stress state for grid RRT is similar to the one recorded for grid R. The only noticeable difference is that the orientation of principal strains and stresses in material space, is about -20° away from the rolling direction of the sheet.</p>	
<p>3rd operation.</p> <p>The strain and stress state for grid RRT is similar to the one recorded for grid R. The only noticeable difference is that the orientation of principal strains and stresses in material space, is about -4° away from the rolling direction of the sheet.</p>	



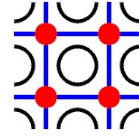
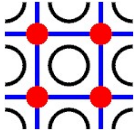
FMTI Systems Inc.

“Forming Measurement Tools Innovations”



IPD application contd.

<p>Description of the deformation evolution in three operations for the Polka Dot grid element, T, located along the transverse direction of the sheet.</p>	<p>Grid analyzer measurements window with the grid image, the FLD displaying apparent major-minor strains, and the principal stress diagram, $\sigma_R - \sigma_T$, which associates the principal stresses with the proximity of their directions to the rolling and transverse directions, R and T, of the sheet.</p>
<p>1st operation.</p> <p>The strain and stress state for grid T is similar to the one recorded for grid R. The only noticeable difference is that the principal strains and stresses associated with directions, R and T, are exchanged.</p>	
<p>2nd operation</p> <p>The strain and stress state for grid T is similar to the one recorded for grid R. The only noticeable difference is that the principal strains and stresses associated with directions, R and T, are exchanged.</p>	
<p>3rd operation.</p> <p>The strain and stress state for grid T is similar to the one recorded for grid R. The only noticeable difference is that the principal strains and stresses associated with directions, R and T, are exchanged.</p>	



Model 200 option SGA2x

The FMTI Grid Analyzer Model 200 option SGA2x targets surface strain measurement based on the digital image analysis by employing a square grid with an approximate size of 1 mm. In comparison with the normal 2.5 mm grid, the 1 mm square grid is more suitable for surface strain measurements in sheet metal forming operations involving deformation localized over a small area such as occurs when wrapping a sheet over a sharp radius, hemming, etc. The development of SGA2x has included an evaluation of the 0.5 mm grid and smaller grids. This evaluation has revealed several serious deficiencies:

- Needs to employ special grid marking techniques to guarantee a required grid consistency (not suitable for marking large surfaces).
- Needs to use sample and camera holding fixtures.
- Ambiguities of measured strain values due to non-uniform evolution of deformation and a possible “orange peel effect noticeable when a small region is magnified.

For the above reasons 1 mm appears to be the reasonable limit to the minimum grid size.

The SGA2x option employs the high-resolution capability of the digital image sensor and the optics of the FMTI grid analyzer model 200 and is derived from the SGA application dedicated primarily for strain measurements using standard 2.5 mm (0.1 inch) square grids. Functionally both the SGA2x and the regular SGA applications are identical, including compensation for surface curvature and capturing strain limits by stitching fractured grids. Figure 1 illustrates the comparison between images of the 1 mm square grid captured by a) SGA and b) SGA2x applications using the same FMTI grid analyzer model 200.

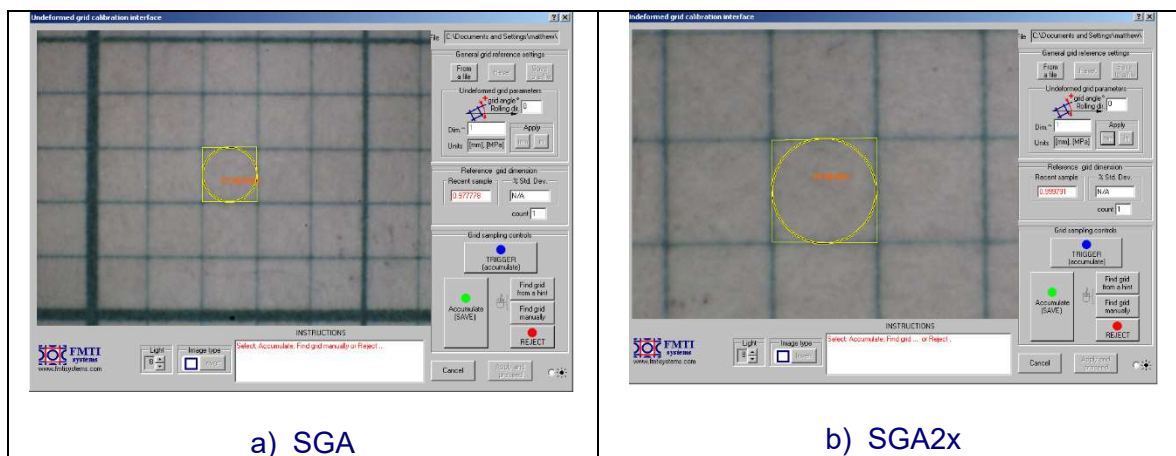


Fig 1 - Comparison between images of a 1 mm square grid

Due to the effect of grid size on the etching quality the accuracy of the measurements of 1 mm square grids may be reduced in the case of relatively thick grid lines or the measurement's efficiency may decrease due to more frequent use of the manual mode to measure grids with incomplete thin lines as shown in figure 2.

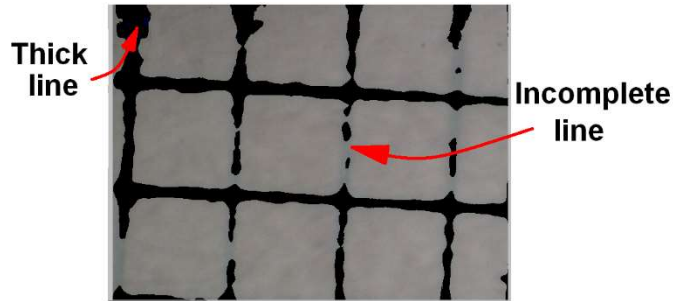
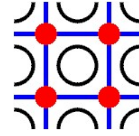
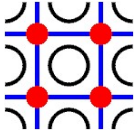
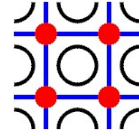
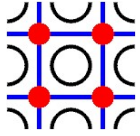


Fig 2 - Deficiencies of grid quality

Our test of ten automatic² measurements using SGA2x with the 1 mm undeformed square grid shown in figure 1b produced the following results:

Same grid element measured 10 times			10 different grid elements taken randomly		
$\epsilon 1$ %	$\epsilon 2$ %	$\epsilon 3$ %	$\epsilon 1$ %	$\epsilon 2$ %	$\epsilon 3$ %
0.8	-1.1	0.3	-0.3	-0.7	1
0.8	-1	0.2	-1.2	-1.3	2.5
0.8	-0.9	0.2	0.7	-2.4	1.8
0.8	-1.2	0.4	0.8	0	-0.8
0.8	-1.1	0.3	1.4	0.9	-2.3
0.8	-1.2	0.4	-1.7	-2.3	4.2
0.8	-1.1	0.3	0.2	-1.4	1.2
0.8	-1.2	0.5	1.8	-0.6	-1.2
0.8	-1	0.2	1.1	-1.8	0.8
0.8	-1	0.3	0.2	-1	0.9

² No use of the manual mode was triggered



Implication Regarding the Usage of a 5mm Circle Grid

The implication of using a 5mm grid versus a 2.5mm ($\frac{1}{4}$ " v. 0.1"), is the inability to detect localized severe deformation in the FLD applications. The following excerpt from the FMTI technical notes illustrates the problem. The image in fig.1 shows the deformed surface of a sheet with the localized groove preceding fracture. The sheet is marked with the 2.5 mm square grid.

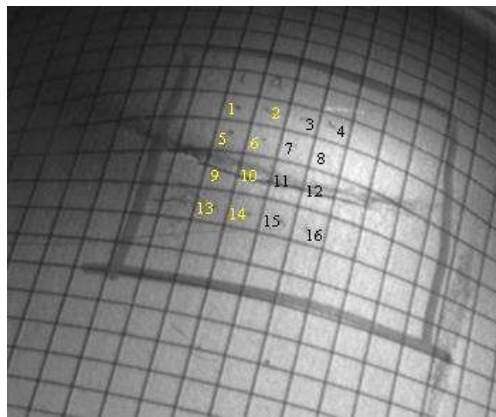


Fig.1

The strain measurements for 16 grid elements taken using the FMTI grid analyzer in the proximity of the critical deformation zone are listed in table 1. If using a single 5 mm circle covering square elements labeled 6,7,10 and 11, the measured stains would be approximately: major strain 31.7%, minor strain 1.7%, indicating that the deformation is just at the boundary of the safe zone on the FLD shown in fig.2.

Table 1

Grid ID	Major engineering % strain	Minor engineering % strain	Thickness engineering % strain
1	14.9	2.7	-15.2
2	14.4	2.2	-14.5
3	14.1	2.1	-14.1
4	14.4	2.3	-14.5
5	22.2	2.4	-20.1
6	20.3	1.7	-18.2
7	19.7	1.9	-18.0
8	20.5	2.6	-19.1
9	42.6	1.8	-31.1
10	43.3	1.6	-31.3
11	43.8	1.6	-31.6
12	43.1	1.9	-31.4
13	18.3	1.3	-16.6
14	19.9	1.4	-17.8
15	20.5	1.0	-17.8
16	19.7	1.4	-17.7

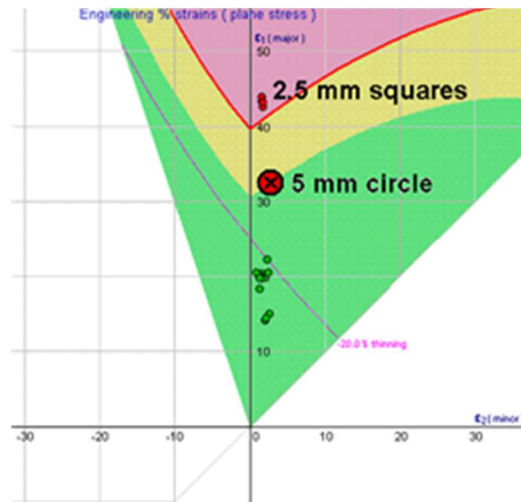
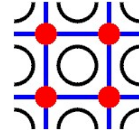
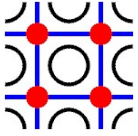


Fig 2

In this case, the measurements performed using a 5mm circle grid would lead to the incorrect conclusion that the deformation is safe.

On the other hand a 5 mm grid can be used in the non-FLD strain measurements in forming applications in which small uniform positive strains of magnitude ~2% are required to produce a smooth surface (for example automotive roofs, doors etc.). In this case, the 5 mm, thin line circle grid, provides the sufficient accuracy needed to detect strains within the 2% range.